J. Fluid Mech. (1968), *vol.* 33, *part* 3, *pp.* 476–493
Printed in Great Britain

Two-dimensional bubbles in slow viscous flows

By S. RICHARDSON†

Department of Applied Mathematics and Theoretical Physics,
University of Cambridge

(Received 12 September 1967)

The representation of a biharmonic function in terms of analytic functions is used to transform a problem of two-dimensional Stokes flow into a boundary-value problem in analytic function theory. The relevant conditions to be satisfied at a free surface, where there is a given surface tension, are derived.

A method for dealing with the difficulties of such a free surface is demonstrated by obtaining solutions for a two-dimensional, inviscid bubble in (*a*) a shear flow, and (*b*) a pure straining motion. In both cases the bubble is found to have an elliptical cross-section.

The solutions obtained can be shown to be unique only if certain restrictive assumptions are made, and if these are relaxed the same methods may give further solutions. Experiments on three-dimensional inviscid bubbles (Rumscheidt & Mason 1961; Taylor 1934) demonstrate that angular points appear in the bubble surface, and an analysis is presented to show that such a discontinuity in a two-dimensional free surface is necessarily a genuine cusp and the nature of the flow about such a point is examined.

1. Introduction

The solution of problems of steady, Newtonian fluid flow involving free surfaces, whether attempted analytically or numerically, presents difficulties arising from the (*a priori*) unknown boundary position. During investigations into such flows, a method was developed which seems to cope with this complication for the case of two-dimensional, slow flows. The method is based on the representation of a biharmonic function by means of analytic functions. This representation is used extensively in plane elasticity theory (Muskhelishvili 1963) and particular mention should be made of a series of papers by Cherepanov (for example, 1963*a*, *b*, 1964) where the method is applied to problems of elastic/plastic behaviour involving an initially unknown elastic domain.

Applications of the technique to two-dimensional Stokes flows with fixed boundaries have been made by a number of authors. Krakowski & Charnes (1953) use the method in a discussion of the Stokes paradox, and a derivation of the basic formulae is given in the book by Langlois (1964). In the context of free surface flows, Clarke (1966, 1968) has used this complex variable formalism in a discussion of the free fall of a viscous jet under gravity. During the course

† Present address: Department of Mathematics, University of Manchester Institute of Science and Technology.

of this work, a paper appeared by Garabedian (1966), where the relevant equations for free surface flows are presented. The solutions there given are obtained by inverse methods and, as with Clarke's work, surface tension is taken to be zero throughout.

Below, the boundary conditions to be satisfied at a free surface where there is a surface tension, T, are derived. The effects of gravity are not included here, but can be incorporated within the scheme as in Clarke (1966). The formulation is then used to solve for the flow around a two-dimensional, inviscid bubble in (a) a shear flow, and (b) a pure straining motion (sometimes referred to as a hyperbolic flow). A discussion of the uniqueness of these solutions and the possibility of the existence of angular points in a two-dimensional free surface is included.

2. Derivation of the equations

Suppose a two-dimensional flow in the Cartesian (x, y)-plane has velocity components (u, v). If the fluid is incompressible, then a streamfunction $\psi(x, y)$ exists such that

$$u = \frac{\partial \psi}{\partial y}; \quad v = -\frac{\partial \psi}{\partial x}. \tag{2.1}$$

For steady flow at zero Reynolds number, ψ satisfies the biharmonic equation and so admits the representation

$$\psi(x, y) = \mathrm{Re}\{\bar{z}\phi(z) + \chi(z)\}, \tag{2.2}$$

where $\phi(z)$ and $\chi(z)$ are functions of the complex variable $z = x + iy$ which are analytic within the flow domain (cf. Muskhelishvili 1963, p. 109). An overbar is here used to denote the complex conjugate.

From this (see Langlois 1964), the velocities are given by

$$-v + iu = \phi(z) + z\overline{\phi'(z)} + \overline{\chi'(z)}, \tag{2.3}$$

the stress components p_{ij} and pressure p (in the absence of body forces) by

$$\left.\begin{aligned} p_{xx} + p_{yy} \equiv -2p &= 8\mu \,\mathrm{Im}\{\phi'(z)\}, \\ i(p_{yy} - p_{xx}) - 2p_{xy} &= 4\mu(\bar{z}\phi''(z) + \chi''(z)), \end{aligned}\right\} \tag{2.4}$$

where μ is the viscosity, and the vorticity ω by

$$\omega = -4\,\mathrm{Re}\{\phi'(z)\}, \tag{2.5}$$

where a prime on a function denotes differentiation with respect to the stated argument.

For the slow motion of any material free from body forces, the divergence of the stress tensor must vanish. This implies (Muskhelishvili, p. 104) the existence of an Airy stress function $U(x, y)$ such that

$$p_{xx} = \frac{\partial^2 U}{\partial y^2}; \quad p_{xy} = -\frac{\partial^2 U}{\partial x \partial y}; \quad p_{yy} = \frac{\partial^2 U}{\partial x^2}. \tag{2.6}$$

U is determined by a given stress field only up to a linear function of x and y. Since the pressure is a harmonic function in Stokes flows, it follows, from (2.4),

that U is a biharmonic function and admits a representation similar to that in (2.2) for ψ. Moreover, comparison with (2.4) shows that this representation can be taken as

$$U = 2\mu \operatorname{Im}\{\bar{z}\phi(z) + \chi(z)\}. \tag{2.7}$$

An examination of (2.3) and (2.4) shows that given velocity and stress fields define $\phi(z)$ and $\chi(z)$ uniquely up to the addition of a term γ_1 to $\phi(z)$ and a term $-\bar{\gamma}_1 z + \gamma_2$ to $\chi(z)$, where γ_1 and γ_2 are complex constants.

Consider now a directed line AB in the fluid. The force $(X_n ds, Y_n ds)$ exerted across a line element ds, *by* fluid on the left *on* fluid on the right, is given by

$$(X_n + iY_n)ds = 2\mu d(\phi(z) - z\overline{\phi'(z)} - \overline{\chi'(z)}). \tag{2.9}$$

This is conveniently derived from (2.7) as in Muskhelishvili (1963, p. 113) or more directly from (2.4) as in Krakowski & Charnes (1953).

Suppose now that AB is a section of the fluid surface at which a surface tension, T, acts, and that there is zero pressure just outside. Then $(X_n ds, Y_n ds)$ is a force of magnitude $T\kappa ds$ directed along the outward normal to the surface, where $\kappa = d\Psi/ds$ is the curvature at that point (see figure 1 for notation). Thus

$$(X_n + iY_n)ds = T\kappa ds(-\sin\Psi + i\cos\Psi) = Td\left[\frac{dz}{ds}\right]. \tag{2.9}$$

Equating this to (2.8) and performing an integration, we obtain the condition to be

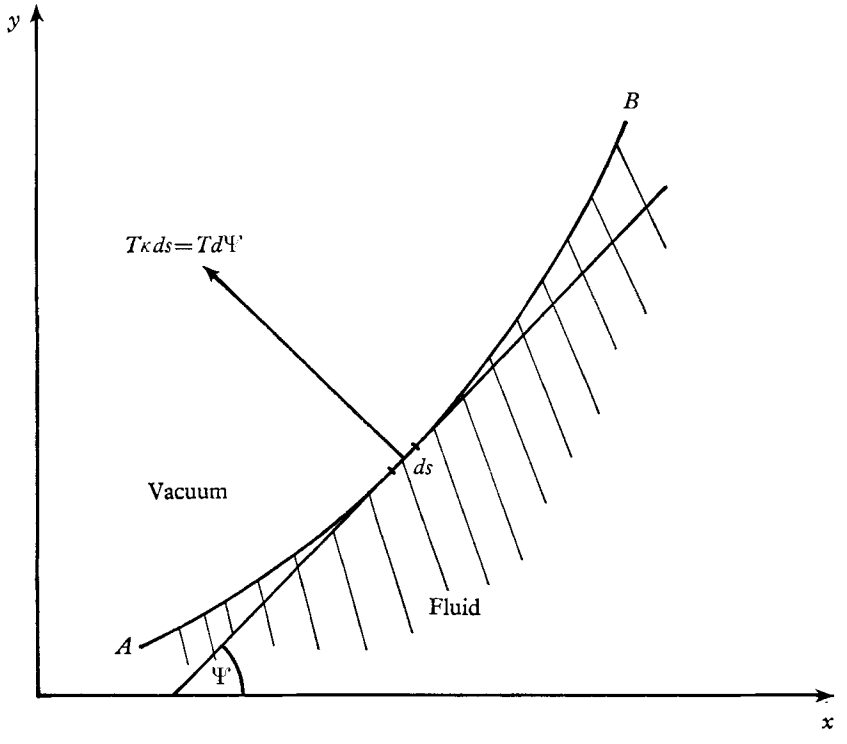

FIGURE 1. Sketch establishing notation for the derivation of the boundary conditions at a free surface.

satisfied at the free surface as

$$\phi(z)-z\overline{\phi'(z)}-\overline{\chi'(z)}=\frac{T}{2\mu}\frac{dz}{\overline{ds}}. \tag{2.10}$$

The constant of integration which arises here can be made to vanish, on *one* free surface, by a suitable choice of γ_1. If more than one free surface is present, there must be constants added to (2.10) for all but one surface and these constants must be determined during the solution. In particular cases, when information is known concerning the forces acting across a line joining two free surfaces, the constants may be related *a priori*, using (2.8).

In steady flow, the surface is also a streamline so that ψ is a constant along it. Differentiating (2.2) along the surface gives

$$\mathrm{Re}\left\{\frac{d\bar{z}}{\overline{ds}}(\phi(z)+z\overline{\phi'(z)}+\overline{\chi'(z)})\right\}=0. \tag{2.11}$$

This can also be seen from (2.3) as a consequence of zero normal velocity at the free surface. (2.10) can now be used to simplify (2.11) to

$$\mathrm{Re}\left\{\frac{d\bar{z}}{\overline{ds}}\phi(z)\right\}=\frac{T}{4\mu}. \tag{2.12}$$

Multiplying (2.10) by $d\bar{z}/ds$ and using (2.12) to eliminate $(d\bar{z}/ds)\phi(z)$ we get

$$\phi(z)\frac{d\bar{z}}{\overline{ds}}+\bar{z}\phi'(z)\frac{dz}{ds}+\chi'(z)\frac{dz}{ds}=0. \tag{2.13}$$

This now integrates to give

$$\bar{z}\phi(z)+\chi(z)=0. \tag{2.14}$$

Here γ_2 has been chosen to make the integration constant vanish on one free surface and similar remarks regarding other possible surfaces apply as for (2.10). Relation (2.14) merely states that both the streamfunction and Airy stress function may be chosen to vanish on one free streamline.

The boundary conditions on the surface will be used in the form of (2.12) and (2.14). Relation (2.3) provides the boundary conditions to be satisfied on a solid surface, so that a problem of two-dimensional Stokes flow can be formulated as a boundary-value problem in analytic functions.

A word of warning is, perhaps, in order concerning these free surface conditions. Their form makes it tempting to regard (2.12) as the 'normal stress condition', with the imaginary part of (2.14) providing the 'zero shear stress condition', but this decomposition is incorrect. It is only possible to deduce (2.14) when the normal stress has the special form demanded by surface tension.

The flow about a two-dimensional bubble involves a doubly connected flow domain with a few consequent complications (Krakowski & Charnes 1953). Suppose this domain comprises the exterior of a simply connected region which contains the origin of the z-plane. Since p and ω represent physical quantities, (2.4) and (2.5) imply that $\phi'(z)$ is single-valued within the flow, so that

$$\phi(z)=A_1\log z+\phi_0(z), \tag{2.15}$$

where A_1 is a complex constant and $\phi_0(z)$ is analytic and single-valued in the flow

region. The single-valued nature of the velocity components then implies, via (2.3), that

$$\chi(z) = \bar{A}_1 z \log z + A_2 \log z + \chi_0(z), \tag{2.16}$$

where A_2 is a complex constant and $\chi_0(z)$ is analytic and single-valued in the flow region. The term multiplying A_2 in $\chi(z)$ gives rise to zero velocity at infinity. However, the terms multiplying A_1 in $\phi(z)$ and $\chi(z)$ give infinite velocities at large distances. The Stokes paradox for a uniform streaming flow past a two-dimensional solid arises because the conditions to be satisfied at the body necessarily imply $A_1 \neq 0$, so preventing the requirements at infinity from being satisfied (see Krakowski & Charnes 1953; Proudman & Pearson 1957; Bretherton 1962). In the case of flow around bubbles this difficulty does not arise and in the following A_1 is taken to vanish.

3. Two-dimensional bubble in a shear flow

Consider now a two-dimensional bubble placed within a shear flow. An axis will exist such that a rotation about it through 180° will leave the situation unchanged. With this point as the origin of the z-plane and the x-axis aligned along the flow direction the situation is as in figure 2.

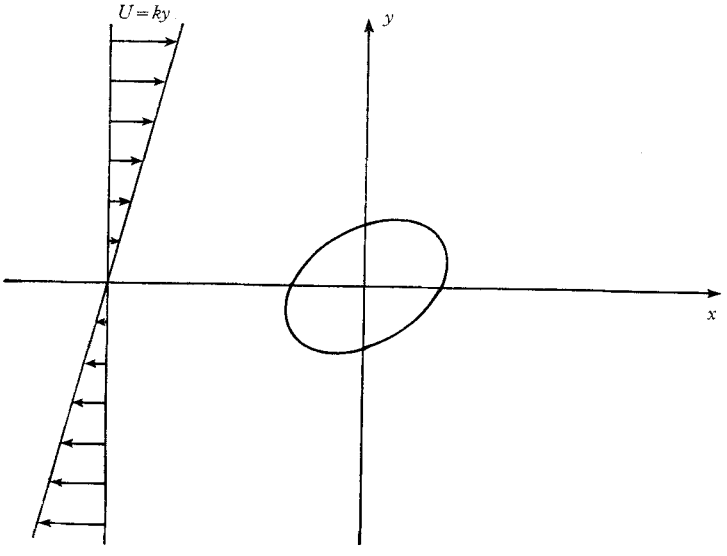

FIGURE 2. Co-ordinate system for the bubble in the shear flow.

With the dominant shear flow at infinity as $(ky, 0)$ this requires

$$\phi(z) \sim \frac{1}{4}\left(k - \frac{ip_\infty}{\mu}\right)z \quad \text{and} \quad \chi(z) \sim -\tfrac{1}{4}kz^2 \quad \text{as} \quad |z| \to \infty, \tag{3.1}$$

where p_∞ is the (unknown) pressure at infinity resulting from zero pressure within the bubble. As $T' \to \infty$ the bubble will become circular and $p_\infty \to -\infty$, so that care needs to be exercised in taking this limit finally, for $\phi(z)$ is then ill-defined.

However, if the physical quantities of interest are first evaluated and then the limit taken, no difficulties arise. This problem could be avoided by taking the pressure within the bubble to be proportional to T, but this is an unnecessary complication, as the free surface conditions are simplified by taking it to be zero. An arbitrary constant pressure superposed on the whole field does not alter the dynamics of the situation, so that the negative pressures which arise here are merely a result of the exploitation of this mathematical simplification and their physical reality is not implied.

By Riemann's theorem, there exists a conformal transformation of the flow region onto the exterior of the unit circle in the ζ-plane, given by $z = w(\zeta)$, where $w(\zeta)$ is analytic in $|\zeta| \geqslant 1$ for a smooth bubble outline. Moreover, this mapping is unique if we require $w(\zeta) \sim a\zeta$ as $|\zeta| \to \infty$ where a is a real constant. a obviously relates to the bubble size and may be regarded as given for the present. The symmetry of the problem implies

$$w(-\zeta) = -w(\zeta). \tag{3.2}$$

Defining
$$\Phi(\zeta) = \phi(w(\zeta)) \quad \text{and} \quad \mathrm{X}(\zeta) = \chi(w(\zeta)), \tag{3.3}$$

these are both analytic functions of ζ in $|\zeta| \geqslant 1$, while

$$\Phi(\zeta) \sim \frac{1}{4}\left(k - \frac{ip_\infty}{\mu}\right)a\zeta \quad \text{and} \quad \mathrm{X}(\zeta) \sim -\tfrac{1}{4}ka^2\zeta^2 \quad \text{as} \quad |\zeta| \to \infty. \tag{3.4}$$

The two boundary conditions (2.14) and (2.12) on the bubble transform into two conditions to be satisfied on the unit circle $|\zeta| = 1$ (Γ say), viz.

$$\overline{w(\zeta)}\,\Phi(\zeta) + \mathrm{X}(\zeta) = 0, \tag{3.5}$$

$$\mathrm{Re}\{i\zeta w'(\zeta)\overline{\Phi(\zeta)}\} = \frac{T}{4\mu}|w'(\zeta)|. \tag{3.6}$$

Equations (3.4), (3.5) and (3.6) are to yield $w(\zeta)$, $\Phi(\zeta)$ and $\mathrm{X}(\zeta)$ in $|\zeta| > 1$ and thence the solution.

If ζ is in the exterior of Γ, then $1/\bar{\zeta}$ is in the interior at the inverse point, and vice versa. As one of them tends to a point on Γ from within, the other tends to that same point from without. Moreover, if $\Omega(\zeta)$ is an analytic function of ζ in the exterior, $\overline{\Omega(1/\bar{\zeta})}$ is an analytic function of ζ in the interior, and vice versa. Consequently, (3.5) implies that the analytic continuation of $w(\zeta)$ into the interior is given by

$$w(\zeta) = -\frac{\overline{\mathrm{X}(1/\bar{\zeta})}}{\overline{\Phi(1/\bar{\zeta})}} \quad \text{for} \quad |\zeta| \leqslant 1. \tag{3.7}$$

From (3.4),
$$w(\zeta) \sim \frac{a}{1-ic}\frac{1}{\zeta} \quad \text{as} \quad |\zeta| \to 0, \tag{3.8}$$

where
$$c = -\frac{p_\infty}{k\mu}.$$

Since there exists the possibility that $\overline{\mathrm{X}(1/\bar{\zeta})}$ has a logarithmic branch point at $\zeta = 0$, it seems, *a priori*, that $w(\zeta)$ could have a branch point there. However, this is not possible for it would necessarily imply a second branch point of $w(\zeta)$,

either in $|\zeta| < 1$ or on $|\zeta| = 1$. The first alternative is untenable because it implies a branch point of $\mathrm{X}(\zeta)$ in $|\zeta| > 1$, and the second because it would make the mapping non-conformal at the bubble surface. It follows, therefore, that the only singularities of $w(\zeta)$, besides the simple poles at $\zeta = 0$ and ∞, are poles at points within Γ such that $\Phi(\zeta)$ has a zero at the inverse point. Also, the logarithmic term in (2.16) for $\chi(z)$ must vanish, i.e. $A_2 = 0$.

Replacing ζ by $1/\bar{\zeta}$ and taking the conjugate in (3.7) we get

$$\mathrm{X}(\zeta) = -\overline{w(1/\bar{\zeta})}\,\Phi(\zeta) \quad \text{throughout} \quad |\zeta| \geqslant 1. \tag{3.9}$$

This now determines $\mathrm{X}(\zeta)$ when $w(\zeta)$ and $\Phi(\zeta)$ are known.

The second condition to be satisfied on Γ, i.e. (3.6), can be written

$$\frac{1}{\zeta}\overline{w'\left(\frac{1}{\bar{\zeta}}\right)}\,\Phi(\zeta) - \zeta w'(\zeta)\overline{\Phi(\zeta)} = \frac{Ti}{2\mu}\left\{w'(\zeta)\overline{w'\left(\frac{1}{\bar{\zeta}}\right)}\right\}^{\frac{1}{2}} \text{ on } \Gamma. \tag{3.6a}$$

This allows $\Phi(\zeta)$ to be analytically continued into $|\zeta| < 1$ exactly as the first condition allowed $w(\zeta)$ to be so continued, and then furnishes the functional relation, valid throughout the ζ-plane,

$$\frac{\Phi(\zeta)}{\zeta w'(\zeta)} - \zeta\frac{\overline{\Phi(1/\bar{\zeta})}}{\overline{w'(1/\bar{\zeta})}} = \frac{Ti}{2\mu}\frac{1}{\{w'(\zeta)\overline{w'(1/\bar{\zeta})}\}^{\frac{1}{2}}}. \tag{3.10}$$

The first term on the left-hand side is analytic and single-valued in $|\zeta| \geqslant 1$, and the second in $|\zeta| \leqslant 1$. The right-hand side has, in general, branch points at the zeros and odd-order poles of $w'(\zeta)$ (all in $|\zeta| < 1$) and at the points inverse to these with respect to the unit circle. If the zeros of $w'(\zeta)$ have even order, the branch points degenerate to poles, but this need not be treated as a special case. Thus the right-hand side of (3.10) can be made analytic in the ζ-plane by introducing two sets of branch cuts—one set in the interior of Γ connecting the zeros and poles of $w'(\zeta)$, and the second set in the exterior connecting those of $\overline{w'(1/\bar{\zeta})}$. Since this right-hand side is $O(1/\zeta)$ as $|\zeta| \to \infty$, a consideration of

$$I_{C_0}(\zeta) = \frac{a}{2\pi i}\int_{C_0}\frac{dt}{(t-\zeta)\{w'(t)\overline{w'(1/\bar{t})}\}^{\frac{1}{2}}}, \tag{3.11}$$

where C_0 is a contour in the t-plane comprising the circle at infinity described anti-clockwise, together with a contour described clockwise around each set of branch cuts of the integrand, gives the decomposition

$$\frac{a}{\{w'(\zeta)\overline{w'(1/\bar{\zeta})}\}^{\frac{1}{2}}} = F_+(\zeta) + F_-(\zeta), \tag{3.12}$$

where

$$\left.\begin{aligned} F_+(\zeta) &= I_{C_-}(\zeta) \quad \text{is analytic in} \quad |\zeta| \geqslant 1, \\ F_-(\zeta) &= I_{C_+}(\zeta) \quad \text{is analytic in} \quad |\zeta| \leqslant 1, \end{aligned}\right\} \tag{3.13}$$

C_- and C_+ being contours around the branch cuts in $|t| < 1$ and $|t| > 1$ respectively, both described clockwise. The flow region corresponds to $|\zeta| > 1$ and, for

ζ in this region, a deformation of contours allows $F_+(\zeta)$ to be written as

$$F_+(\zeta) = -\frac{a}{2\pi i}\int_{\Gamma'} \frac{dt}{(t-\zeta)\overline{|w'(t)|}}, \tag{3.14}$$

where Γ' is the unit circle in the t-plane traversed anti-clockwise. Writing $t = e^{i\theta}$ allows this integral to be simply put in terms of real integrals. A similar deformation gives

$$F_-(0) = \frac{a}{2\pi i}\int_{\Gamma'} \frac{dt}{t\overline{|w'(t)|}}, \tag{3.15}$$

and again a simple evaluation is possible. (3.10) can now be written as

$$\frac{\Phi(\zeta)}{\zeta w'(\zeta)} - \frac{Ti}{2\mu a}F_+(\zeta) = \zeta\overline{\frac{\Phi(1/\bar{\zeta})}{w'(1/\bar{\zeta})}} + \frac{Ti}{2\mu a}F_-(\zeta). \tag{3.16}$$

The left-hand side is analytic in $|\zeta| \geqslant 1$ and tends to $\frac{1}{4}k(1+ic)$ as $|\zeta| \to \infty$. The right-hand side is analytic in $|\zeta| \leqslant 1$ and tends to $\frac{1}{4}k(1-ic) + (Ti/2\mu a)F_-(0)$ as $|\zeta| \to 0$.

It follows, by Liouville's theorem, that both sides are equal to one and the same constant, so that

$$\frac{\Phi(\zeta)}{\zeta w'(\zeta)} = \frac{k}{4}(1+ic) + \frac{Ti}{2\mu a}F_+(\zeta), \tag{3.17}$$

and

$$c = \frac{T}{a\mu k}F_-(0). \tag{3.18}$$

Equation (3.17) determines $\Phi(\zeta)$ when $w(\zeta)$ is known and (3.18) provides a restriction on $w(\zeta)$. Note that the definitions imply that

$$\overline{F_+(1/\bar{\zeta})} = F_-(\zeta) - F_-(0), \tag{3.19}$$

so that (3.17) follows from putting either side of (3.16) equal to the constant.

For infinite surface tension, the bubble may be expected to become circular, with only the zero shear stress condition applicable at its surface. This problem can be solved by a straightforward separation of the variables in the biharmonic equation and leads to the solution

$$\psi = \tfrac{1}{4}k(r^2 - a^2)(1 - \cos 2\theta), \tag{3.20}$$

where (r, θ) are the usual polar co-ordinates. When translated into the complex variable form, this yields no zeros of $\Phi(\zeta)$ in $|\zeta| \geqslant 1$. In fact, bearing in mind that $p_\infty \to -\infty$ in this limit, condition (3.4) alone implies that the only zeros of $\Phi(\zeta)$ are then at the origin.

The opposite extreme of zero surface tension, when the bubble degenerates to a slit along the real axis, can also be solved separately (appendix A) and gives a pair of zeros of $\Phi(\zeta)$ just on the unit circle at $\zeta = \pm 1$ (corresponding to the cusps on the bubble), coinciding with zeros of $X(\zeta)$.

It would therefore seem reasonable, in the general case, to expect a solution in which $\Phi(\zeta)$ has no zeros in $|\zeta| > 1$.† It then follows that $w(\zeta)$ has

† This condition is not, in fact, essential for the validity of the solution to be obtained. The method of construction ensures that any zeros of $\Phi(\zeta)$ in $|\zeta| \geqslant 1$ coincide with zeros of $X(\zeta)$.

the form $$w(\zeta) = a(\zeta + \gamma^2/\zeta), \quad \text{where} \quad \gamma^2 = \frac{1}{1-ic}. \tag{3.21}$$

$|\gamma|^2 < 1$ ensures that the mapping is conformal in the flow domain. (3.15) is then

$$F_-(0) = -\frac{1}{2\pi}\int_{\Gamma'} \frac{dt}{(\gamma^2 - t^2)^{\frac{1}{2}}(1-\overline{\gamma}^2 t^2)^{\frac{1}{2}}}. \tag{3.22}$$

Transforming by $\gamma s = t$, deforming the contour in the s-plane to run either side of the branch cut from -1 to $+1$, and using the symmetry properties of the integrand we have

$$F_-(0) = (2/\pi)K(|\gamma|^2), \tag{3.23}$$

where $K(m)$ is the complete elliptic integral of the first kind defined by

$$K(m) = \int_0^1 \frac{ds}{(1-s^2)^{\frac{1}{2}}(1-m^2 s^2)^{\frac{1}{2}}}. \tag{3.24}$$

This function is tabulated with argument m^2 in most of the standard tables of mathematical functions (e.g. Jahnke, Emde & Lösch 1960), while Fletcher (1940) tabulates with argument m. Incidentally, the reverse procedure, expressing $K(m)$ in a form similar to (3.22), would seem to be an ideal method for evaluating it numerically, as this avoids the singularity of the integrand in (3.24) on the path of integration.

Equation (3.18) now assumes the form

$$c = \frac{2T}{\pi a \mu k} K([1+c^2]^{-\frac{1}{2}}). \tag{3.25}$$

The function $K([1+c^2]^{-\frac{1}{2}})$ is sketched in figure 3, from which it can be seen that (3.25) has just one root c for each value of the surface tension parameter $Z = T/a\mu k$. For $Z > 0$, this gives $c > 0$; i.e. a positive surface tension implies negative pressures at infinity. As $Z \to \infty$, then $c \to \infty$ and $\gamma^2 \to 0$ so that the bubble becomes circular. As $Z \to 0$, then $c \to 0$ and $\gamma^2 \to 1$ so that the bubble becomes a slit.

The mapping (3.21) with $\gamma^2 = \rho e^{2i\phi}$ gives an ellipse with its major axis inclined at an angle ϕ to the flow direction, and a deformation $D = \rho$, where

$$D = \frac{\text{major axis} - \text{minor axis}}{\text{major axis} + \text{minor axis}}. \tag{3.26}$$

The special form of γ^2 implies that it lies in the upper half of the complex plane on the semi-circle with diameter the segment (0, 1) of the real axis so that

$$D = \cos 2\phi. \tag{3.27}$$

A sketch of the streamlines for the case $c = 3$, corresponding to $Z = 2{\cdot}923$, $D = 0{\cdot}316$, $\phi = 36°$, is given in figure 4. The streamlines are contoured at equal intervals of the square root of the non-dimensional streamfunction ψ/ka^2, and the pattern here is typical for other values of Z. In particular, there are two zero

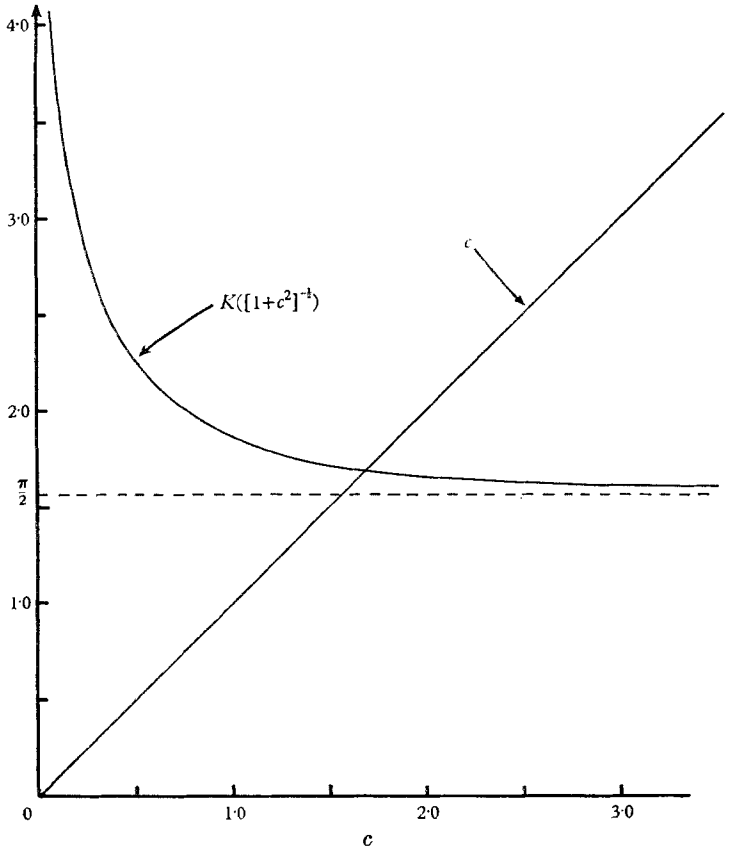

FIGURE 3. Variation of the function $K([1+c^2]^{-\frac{1}{2}})$.

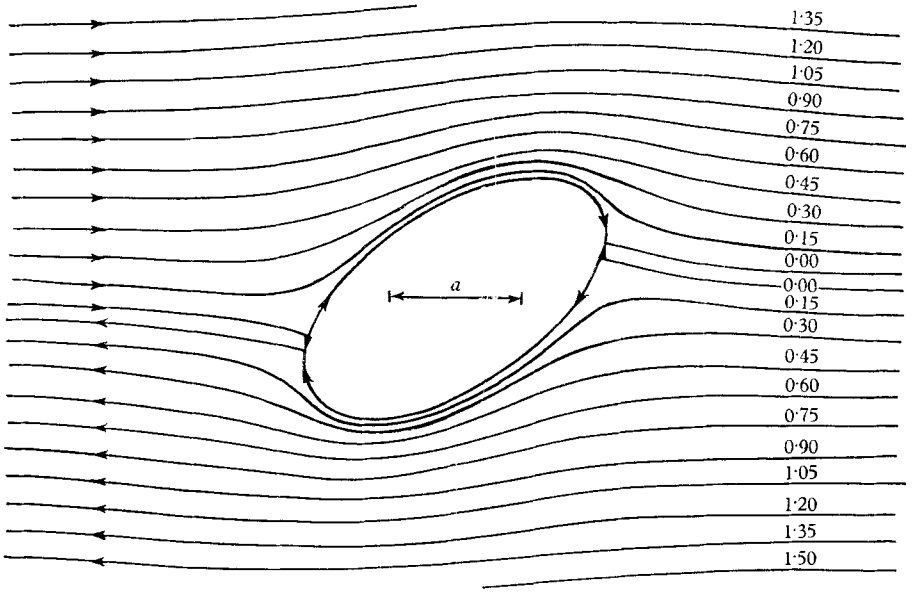

FIGURE 4. Sketch of the streamlines around a bubble in a shear flow for the case $c = 3$, corresponding to $Z = 2{\cdot}923$, $D = 0{\cdot}316$, $\phi = 36°$. The streamlines are drawn at equal increments of the square root of the streamfunction, the numbers giving the value of $(\psi/ka^2)^{\frac{1}{2}}$.

streamlines on each side of the bubble and these enclose a (very weak) circulation. In the limits $Z \to 0$ and $Z \to \infty$, these streamlines coalesce. Further details are given in appendix C.

4. Two-dimensional bubble in a pure straining motion

Consider now the two-dimensional bubble placed at the origin in the pure straining motion $\mathbf{u} = (Cx, -Cy)$, where $C > 0$. Such a flow is equivalent to a rigid rotation superposed on a simple shear of magnitude $k = 2C$, so that, for nearly circular bubbles, there is an equivalence with the preceding problem (cf. Taylor 1934).

Now, with a notation paralleling that of §3,

$$\phi(z) \sim -\frac{ip_\infty}{4\mu} z; \quad \chi(z) \sim -\frac{iC}{2} z^2 \quad \text{as} \quad |z| \to \infty. \tag{4.1}$$

Proceeding exactly as before, the mapping will now have the symmetries

$$w(\zeta) = -w(-\zeta) = \overline{w(\bar{\zeta})}. \tag{4.2}$$

In the ζ-plane,

$$\Phi(\zeta) \sim -\frac{ip_\infty}{4\mu} a\zeta; \quad \mathrm{X}(\zeta) \sim -\frac{iC}{2} a^2\zeta^2 \quad \text{as} \quad |\zeta| \to \infty. \tag{4.3}$$

The continuation of $w(\zeta)$ into the interior of Γ now yields

$$w(\zeta) \sim -\frac{2aC\mu}{p_\infty \zeta} \quad \text{as} \quad |\zeta| \to 0. \tag{4.4}$$

At large distances

$$\frac{\Phi(\zeta)}{\zeta w'(\zeta)} \sim -\frac{ip_\infty}{4\mu} \quad \text{as} \quad |\zeta| \to \infty, \tag{4.5}$$

so that (3.17) and (3.18) are replaced by

$$\frac{\Phi(\zeta)}{\zeta w'(\zeta)} = -\frac{ip_\infty}{4\mu} + \frac{Ti}{2\mu a} F_+(\zeta), \tag{4.6}$$

and

$$-p_\infty = \frac{T}{a} F_-(0). \tag{4.7}$$

Again the two limiting cases can be evaluated separately. The circular bubble at infinite surface tension gives

$$\psi = \tfrac{1}{2}C(r^2 - a^2)\sin 2\theta. \tag{4.8}$$

The zero surface tension limit in this case is very simple, for the basic straining motion transmits only a constant normal force across the real axis, so that the bubble is again a slit along this axis with no perturbation on the flow. In this limit, the governing equations are invariant under a reversal of the velocities, so that there is also a solution with the bubble as a slit along the imaginary axis, but this is evidently a singular solution.

In both these limiting cases the solutions in terms of complex variables show no zeros of $\Phi(\zeta)$ in $|\zeta| > 1$ so that $w(\zeta)$ in general can be expected to have the form

$$w(\zeta) = a\left(\zeta + \frac{\gamma^2}{\zeta}\right) \quad \text{where} \quad \gamma^2 = -\frac{2C\mu}{p_\infty} \quad \text{is real,} \tag{4.9}$$

so that the bubble is an ellipse aligned along the real axis.

Equation (4.7) now determines γ^2 by

$$\frac{1}{\gamma^2} = \frac{T}{\pi a \mu C} K(\gamma^2). \tag{4.10}$$

The sketch of $K(\gamma^2)$ in figure 5 shows that this has just one root for each value of the surface tension parameter $Z = T/2a\mu C$ and that the behaviour at the extremes of Z is as expected. Moreover, $p_\infty \leqslant -2C\mu$ for all positive values of Z.

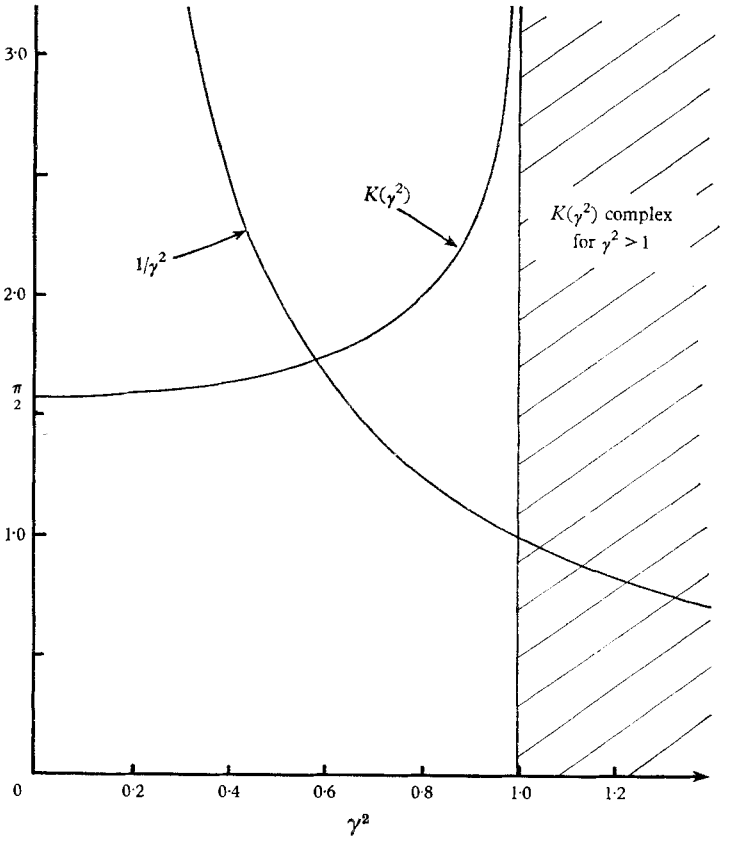

FIGURE 5. Variation of the function $K(\gamma^2)$.

The streamlines for the case $\gamma^2 = D = 0{\cdot}3$ are sketched in figure 6, and a discussion of the behaviour at large distances is contained in appendix B.

Comparison of (3.25) and (4.10) shows the expected similarity of behaviour for nearly circular bubbles, but the behaviours at the other extreme are very different. From (3.25), $ZK(D) \to 0$ as $Z \to 0$ for the shear flow, but from (4.10), $ZK(D) \to \frac{1}{2}\pi$

as $Z \to 0$ for the straining motion. Thus, in the latter case, care is needed in extracting this limit from the solution; for example, the second term on the right-hand side of (4.6) does not vanish.

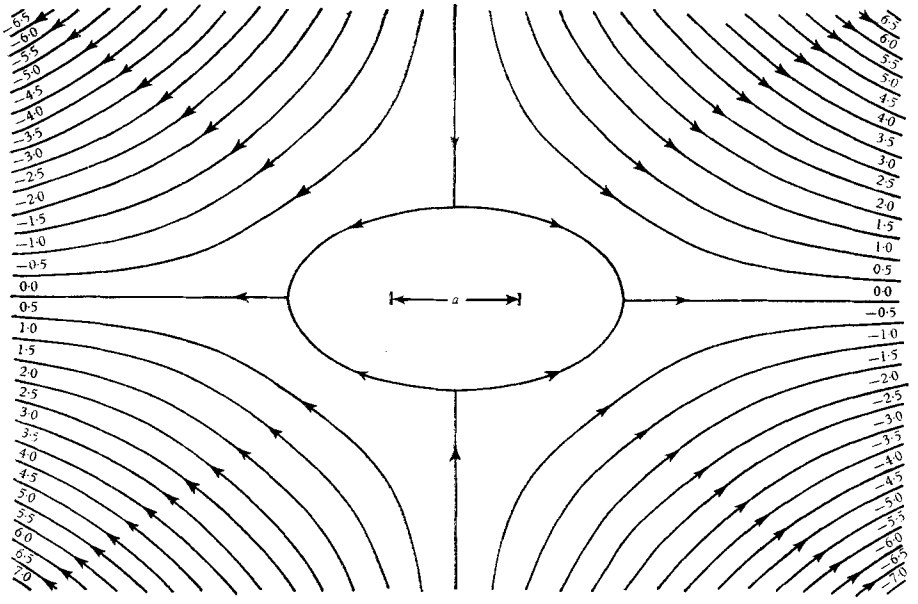

FIGURE 6. Sketch of the streamlines around a bubble in a pure straining motion for the case $D = 0{\cdot}3$ corresponding to $Z = 3{\cdot}256$. The streamlines are drawn at equal increments of the streamfunction, the numbers giving the value of ψ/Ca^2.

5. The parameter a

In the preceding sections, the bubble size has been determined by the parameter a. From the theoretical point of view this is the obvious length scale to use, but in a given situation it does not correspond directly to any given length, although it differs from the semi-major axis by at most a factor of 2. However, any conveniently measured length can always be simply related to a. Suppose, for example, that, in the straining motion, the semi-major axis L is measured. Then a is determined by L, and vice versa, through

$$\frac{a^2}{L-a} = \frac{1}{\pi}\frac{T}{\mu C} K\left(\frac{L-a}{a}\right) \tag{5.1}$$

once the length $T/\mu C$ is known. (5.1) has just one root such that $a \leqslant L \leqslant 2a$.

6. Concerning observations on three-dimensional bubbles

Experiments on three-dimensional bubbles by Taylor (1934) and Rumscheidt & Mason (1961) in the two flow situations discussed here, show similarities of behaviour, but, as is to be expected, there is no quantitative agreement. A major qualitative difference concerns the appearance of angular points or cusps in the

bubble surface when the fluid velocities exceed a critical value. *A priori*, these could arise from (i) three-dimensional effects, (ii) higher Reynolds number effects, (iii) non-uniqueness of the solution.

Consider the situation at a theoretical angular point of a free surface in a two-dimensional, slow flow, with axes and notation as in figure 7. An examination of the flow about such a point has been carried out by Moffatt (1964) with a neglect

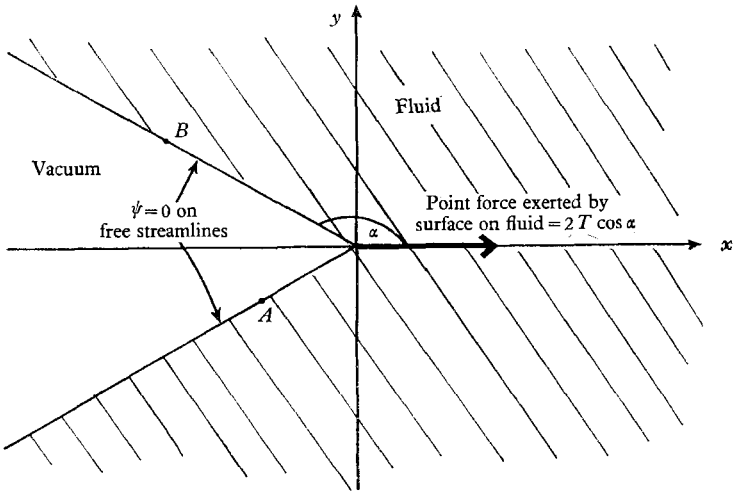

FIGURE 7. Sketch establishing notation for the discussion of behaviour at an angular point.

of the normal stress condition, on the assumption that the motion of a relatively inviscid fluid adjacent to the surface could provide the normal stresses necessary to give a balance.

Boundary condition (2.14) implies that

$$\begin{aligned} e^{-2i\alpha} z\phi(z) + \chi(z) &= 0 \quad \text{on} \quad \arg z = \alpha \\ e^{2i\alpha} z\phi(z) + \chi(z) &= 0 \quad \text{on} \quad \arg z = -\alpha. \end{aligned} \tag{6.1}$$

These two requirements are compatible only if

$$\alpha = \tfrac{1}{2}n\pi \quad \text{for integral } n. \tag{6.2}$$

This shows that a discontinuity in a free surface is necessarily a genuine cusp ($\alpha = 0$ or π). In this context it should be noted that the remarks in Garabedian's (1966) paper, following equation (65), purporting to give a solution corresponding to a discontinuity with $\alpha = \frac{1}{4}\pi$, are incorrect.

In the neighbourhood of the cusp (6.1) implies

$$\chi(z) = -z\phi(z). \tag{6.3}$$

Because of the surface discontinuity it is convenient to apply the remaining boundary condition by using the integrated form of (2.8). With A and B points on the lower and upper surfaces respectively, this gives

$$\left[\phi(z) - z\overline{\phi'(z)} - \overline{\chi'(z)}\right]_A^B = \pm T/\mu, \tag{6.4}$$

where the left-hand side denotes the difference in the bracketed quantity at B and A, while on the right-hand side the positive and negative signs correspond to $\alpha = 0$ and $\alpha = \pi$ respectively.

Using (6.3) this becomes

$$\left[\mathrm{Re}\{\phi(z)\}\right]_A^B = \pm T/2\mu. \tag{6.5}$$

This requirement excludes the possibility $\alpha = 0$ (except for an obviously singular solution at $T = 0$), and for $\alpha = \pi$ implies a behaviour near the point as

$$\phi(z) = \frac{Ti}{4\pi\mu} \log z. \tag{6.6}$$

In terms of the usual polar co-ordinates (r, θ), with $\theta = 0$ along the positive x-axis, this gives

$$\psi = \frac{T}{2\pi\mu} r \log r \sin\theta. \tag{6.7}$$

Note that this term gives rise to velocities near the point which are in the *negative* x-direction. The radial normal stress component is given by

$$p_{rr} = \frac{2T}{\pi} \frac{\cos\theta}{r}, \tag{6.8}$$

and an integration around a circle centred on the origin shows how the flow produces the δ-function behaviour of the force per unit free surface length to balance the surface tension forces.

It should be noted that the logarithmic term needed in the local expansion (6.6) is not excluded by the absence of the logarithmic terms from (2.16). As pointed out to me by Dr F. P. Bretherton, the analogous three-dimensional situation is rather different, for the surface is now approximately conical and the surface tension forces per unit area vary as the inverse power of the distance from the point (see Taylor 1964).

At any Reynolds number, an expansion in the neighbourhood of a given point necessarily involves the Stokes equations as a first approximation, so that the above deduction that any discontinuity must be a genuine cusp remains valid. In practice, of course, when the surface becomes cusp-like the material filling the bubble must begin to affect the dynamics at this point, no matter how small may be its viscosity compared with that of the surrounding medium.

The solutions obtained above are unique under the assumption that they are to vary continuously with a change in the governing parameter Z, and that the limit $Z \to \infty$ is the expected circular cylinder. Any further solutions must have zeros of $\phi(z)$ within the flow field and may have cusps at the boundary. The above methods will give such solutions by relaxing some of the conditions imposed, but they can only be reached from the given solution curves by a discontinuous jump, presumably as the result of an instability. In connexion with this, Rumscheidt & Mason remark that the transition from rounded to pointed ends in their experiments appeared to occur suddenly.

7. Concluding remarks

While the flow fields obtained about the bubbles are correct solutions to the Stokes equations, they do not represent uniformly valid approximations to solutions of the full Navier–Stokes equations. The situation is, however, less disastrous than the analogous case of a rigid cylinder in a uniform stream, when there is no solution to the Stokes equations satisfying all the boundary conditions on the body and at infinity. Here, the dominant velocities at infinity are of order r, while the perturbation velocities are of order $1/r$ (see appendixes B and C), so that the ratio of the inertial to viscous terms in the full equation of motion is $R(r/a)^2$, where R is a suitably defined Reynolds number. The solutions obtained strictly hold only out to a radius $o(aR^{-\frac{1}{2}})$ and are evidently the first terms of an inner expansion of a matched asymptotic expansion procedure.

The author would like to thank Dr H. K. Moffatt for advice on the preparation of this paper, and Dr A. B. Tayler, whose remarks first led to the inclusion of surface tension in the formulation of §2. The numerical work involved in the production of figures 4, 6 and 8 was carried out on the TITAN computer at the University Mathematical Laboratory, Cambridge. This research was carried out while in receipt of an S.R.C. Research Studentship.

Appendix A. The zero surface tension limit for the bubble in the shear flow

For the bubble in the shear flow at zero surface tension the solution is

$$\left.\begin{aligned} w(\zeta) &= a\left(\zeta+\frac{1}{\zeta}\right), \\ \Phi(\zeta) &= \frac{k}{4}a\left(\zeta-\frac{1}{\zeta}\right), \\ \mathrm{X}(\zeta) &= -w(\zeta)\,\Phi(\zeta). \end{aligned}\right\} \tag{A 1}$$

Reverting to the z-plane, the bubble has become the slit $(-2a, 2a)$ on the real axis and

$$\left.\begin{aligned} \phi(z) &= \tfrac{1}{4}k(z^2-4a^2)^{\frac{1}{2}}, \\ \chi(z) &= -\tfrac{1}{4}kz(z^2-4a^2)^{\frac{1}{2}}, \end{aligned}\right\} \tag{A 2}$$

where the root varying as z at large distances is chosen in each case.

An examination of this solution shows that the velocities vanish on the segments of the real axis, $|x| > 2a$, so that, considering just the half of the flow field in $y > 0$, this furnishes the solution with a shear flow over a slot in a plane wall. The free surface from $-2a$ to $+2a$ is now plane, so that this is a solution for any value of the surface tension, provided only that the pressures at infinity and just outside the free surface are equal. A sketch of the flow is given in figure 8.

A local expansion about the point $z = 2a$ using the usual polar co-ordinates (r, θ), with $\theta = 0$ on the fixed surface $x > 2a$, shows that the dominant term in

the streamfunction near this point is

$$\psi = ka^{\frac{1}{2}}r^{\frac{3}{2}}\sin\theta\sin\tfrac{1}{2}\theta, \tag{A 3}$$

agreeing with the analysis performed by Michael (1958) of the flow in the neighbourhood of such a singularity. The flow about $z = -2a$ is, of course, of similar form.

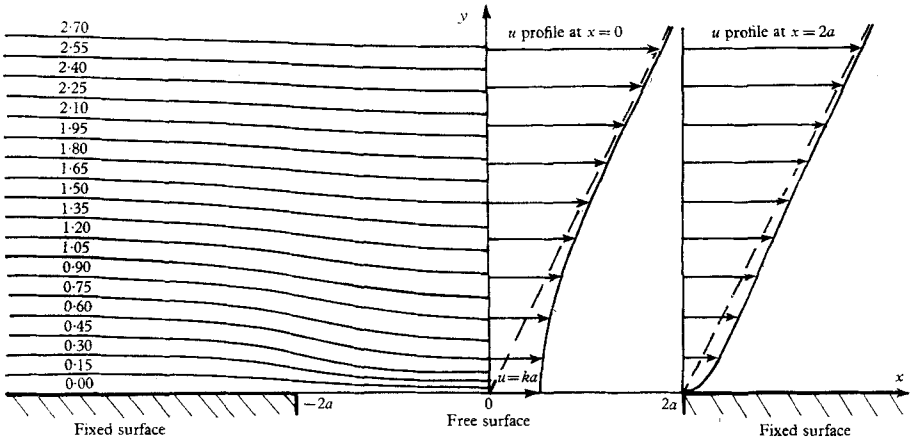

FIGURE 8. Sketch of the shear flow over a slot in a plane wall when the pressure at large distances in the flow is equal to the pressure just outside the free surface. The flow has a symmetry about the y-axis. The streamlines are drawn on the left at equal increments of the square root of the streamfunction, the numbers giving the value of $(\psi/ka^2)^{\frac{1}{2}}$. The velocity profiles at $x = 0$ and $x = 2a$ are plotted on the right with a velocity ka represented by a length $\frac{1}{2}a$.

Appendix B. The behaviour at large distances for the bubble in the straining motion

Defining

$$A = \frac{2}{\pi}\int_0^1 \frac{s^2\,ds}{(1-s^2)^{\frac{1}{2}}(1-\gamma^4 s^2)^{\frac{1}{2}}} = \frac{2}{\pi\gamma^4}\{K(\gamma^2)-E(\gamma^2)\}, \tag{B 1}$$

where $E(m)$ is the complete elliptic integral of the second kind defined by

$$E(m) = \int_0^1 \frac{(1-m^2s^2)^{\frac{1}{2}}}{(1-s^2)^{\frac{1}{2}}}\,ds, \tag{B 2}$$

an expansion for large $|z|$ yields

$$\left.\begin{aligned}\phi(z) &= \frac{iC}{2\gamma^2}z + i\left(\frac{A\gamma^2Ta}{2\mu} - Ca^2\right)\frac{1}{z} + O\left(\frac{1}{z^3}\right),\\ \chi(z) &= -\frac{iC}{2}z^2 + i\left(\frac{3Ca^2\gamma^2}{2} - \frac{Ca^2}{2\gamma^2} - \frac{A\gamma^4Ta}{2\mu}\right) + O\left(\frac{1}{z^2}\right).\end{aligned}\right\} \tag{B 3}$$

The first terms here give the required straining motion, while the second add to the streamfunction a term

$$\left(\frac{ATa\gamma^2}{2\mu} - Ca^2\right)\sin 2\theta. \tag{B 4}$$

For $\gamma^2 = 1$ this term vanishes, while for $\gamma^2 \to 0$ it becomes $-\frac{1}{2}Ca^2 \sin 2\theta$ (cf. (4.8)). For intermediate values, the coefficient of $\sin 2\theta$ is always negative so that the perturbation velocities at infinity are of order Ca^2/r and represent a radial outflow in the quadrants $-\frac{1}{4}\pi < \theta < +\frac{1}{4}\pi$ and $\frac{3}{4}\pi < \theta < \frac{5}{4}\pi$ with an inflow elsewhere.

Appendix C. The streamlines for the bubble in the shear flow

An analysis of the flow at large distances in the shear flow can be carried out as in appendix B for the straining motion.

Defining now

$$B = \frac{2}{\pi}\int_0^1 \frac{s^2 ds}{(1-s^2)^{\frac{1}{2}}(1-|\gamma|^4 s^2)^{\frac{1}{2}}} = \frac{2}{\pi|\gamma|^4}\{K(|\gamma|^2) - E(|\gamma|^2)\}, \tag{C 1}$$

there results, for large $|z|$,

$$\left.\begin{aligned} \phi(z) &= \frac{k}{4\bar{\gamma}^2}z + \left(\frac{BTi}{2\mu} - \frac{ka}{2\bar{\gamma}^2}\right)a\gamma^2\frac{1}{z} + O\left(\frac{1}{z^3}\right), \\ \chi(z) &= -\frac{k}{4}z^2 + \left(\frac{ka^2}{4}\left\{3\gamma^2 - \frac{1}{\bar{\gamma}^2}\right\} - \frac{BT|\gamma|^4 ai}{2\mu}\right) + O\left(\frac{1}{z^2}\right). \end{aligned}\right\} \tag{C 2}$$

The first terms give the required shear flow, while the second term in $\phi(z)$ gives radial velocities decaying as $1/r$, as for the straining motion, but not now aligned along the axes. Of greater interest here is the behaviour as $x \to \pm\infty$ for fixed y. In this limit

$$\psi = \tfrac{1}{2}ky^2 + \frac{ka^2c^2}{2}\left[\frac{E(|\gamma|^2)}{K(|\gamma|^2)} - 1 + \tfrac{1}{2}|\gamma|^4\right]. \tag{C 3}$$

The added constant term vanishes only at the limits $|\gamma|^2 = 1$ and $|\gamma|^2 = 0$ and for other values the bracketed quantity is strictly negative. The numerical value of this added term is $-0{\cdot}00296ka^2$ for the particular case, $c = 3$, plotted in figure 4, and the numerical coefficient here is always small. It follows that two zero streamlines move off to infinity in both positive and negative x-directions.

A straightforward expansion of the streamfunction in terms of a local radial co-ordinate δ, about a point on the bubble surface, shows that, if n zero streamlines join the surface at that point, this expansion has a dominant term $O(\delta^{n+1})$. In particular, one zero streamline gives rise to a dominant term $O(\delta^2)$ and it must meet the surface at right angles.

The streamfunction can be written as

$$\psi = \mathrm{Re}\left\{\left[\overline{w(\zeta)} - \overline{w\left(\frac{1}{\bar{\zeta}}\right)}\right]\Phi(\zeta)\right\}. \tag{C 4}$$

Writing $\zeta = e^{i\beta} + \xi$ where $|\xi| \ll 1$ and performing an expansion for small $|\xi|$ we obtain

$$\zeta w'(\zeta)\left[\overline{w(\zeta)} - \overline{w\left(\frac{1}{\bar{\zeta}}\right)}\right] = 2a^2|1-\gamma^2 e^{-2i\beta}|^2\,\mathrm{Re}\{e^{-i\beta}\xi\} + O(\xi^2). \tag{C 5}$$

It follows from (3.17) that points where a zero streamline joins the bubble

correspond to values of β given by the roots of

$$\frac{a\mu k}{2T} = \mathrm{Im}\{F_+(e^{i\beta})\}. \tag{C 6}$$

This equality can be written more symmetrically as

$$\mathrm{Im}\left\{\int_0^1 \frac{ds}{(1-\gamma^2)(1-s^2)^{\frac{1}{2}}(1-|\gamma|^4 s^2)^{\frac{1}{2}}}\right\}$$
$$= \tfrac{1}{2}\,\mathrm{Im}\left\{\int_0^1 \frac{ds}{(1-\gamma^2 e^{-2i\beta}s^2)(1-s^2)^{\frac{1}{2}}(1-|\gamma|^4 s^2)^{\frac{1}{2}}}\right\}. \tag{C 7}$$

Numerical work shows that this always has just four roots: two near $\beta = 0$ and two symmetrically placed near $\beta = \pi$. The streamlines must thus behave as in figure 4. In the limits when $\gamma^2 \to 1$ or 0 the four roots coalesce to two at $\beta = 0$ and π.

For the sketches of figures 4 and 6, $F_+(\zeta)$ was evaluated in the form (3.14). This has the disadvantage that, if any grid points lie close to the bubble surface, a straightforward numerical integration here may give a poor approximation. However, this gave no trouble; as a check, the formulae were used to provide values of the streamfunction within the bubble, so that the plotting routine could be allowed to interpolate for the zero streamline of the bubble surface, and this gave the ellipse to the accuracy adopted in the working. A more satisfactory procedure would be to leave the integrand of $F_+(\zeta)$ in the form of (3.11) and deform the contour in the t-plane to a circle of radius less than unity and just greater than $|\gamma|$, but this then requires the extraction of complex square roots, a much more time-consuming process numerically than the extraction of the real roots involved with (3.14).

REFERENCES

Bretherton, F. P. 1962 *J. Fluid Mech.* **12**, 591.

Cherepanov, G. P. 1963*a* *P.M.M.* **27**, 275.

Cherapanov, G. P. 1963*b* *P.M.M.* **27**, 428.

Cherepanov, G. P. 1964 *P.M.M.* **28**, 141.

Clarke, N. S. 1966 Ph.D. Thesis, London University.

Clarke, N. S. 1968 *J. Fluid Mech.* **31**, 481.

Fletcher, A. 1940 *Phil. Mag.* (7), **30**, 516.

Garabedian, P. R. 1966 *Comm. Pure Appl. Math.* **19**, 421.

Jahnke, E., Emde, F. & Lösch, F. 1960 *Tables of Higher Functions.* New York: McGraw-Hill.

Krakowski, M. & Charnes, A. 1953 Stokes' paradox and biharmonic flows. *Carnegie Institute of Technology, Technical Rept.* no. 37.

Langlois, W. E. 1964 *Slow Viscous Flow.* New York: Macmillan.

Michael, D. H. 1958 *Mathematika*, **5**, 82.

Moffatt, H. K. 1964 *J. Fluid Mech.* **18**, 1.

Muskhelishvili, N. I. 1963 *Some Basic Problems of the Mathematical Theory of Elasticity.* Translated by J. R. M. Radok. P. Noordhoff Ltd.

Proudman, I. & Pearson, J. R. A. 1957 *J. Fluid Mech.* **2**, 237.

Rumscheidt, F. D. & Mason, S. G. 1961 *J. Colloid Sci.* **16**, 238.

Taylor, G. I. 1934 *Proc. Roy. Soc.* A **146**, 501.

Taylor, G. I. 1964 *Proceedings of the 11th International Congress of Applied Mechanics.* Editor, H. Görtler. Munich: Springer Verlag.